Transactions of the **13th International Conference on Structural Mechanics in Reactor Technology** (SMiRT 13), Escola de Engenharia - Universidade Federal do Rio Grande do Sul, Porto Alegre, Brazil, August 13-18, 1995

Shear wall ultimate drift limits for PRA applications

Duffey, T.A. [1], Farrar, C.R. [2], Goldman, A. [2]
1) New Mexico Highlands University, Las Vegas, New Mexico, USA
2) Los Alamos National Laboratory, Los Alamos, New Mexico, USA

ABSTRACT: Drift limits for reinforced concrete shear walls are investigated by reviewing the technical literature for appropriate experimental data. Based on the geometry of actual nuclear power plant structures (exclusive of containments) and concerns regarding their response during seismic loading, data are obtained from pertinent references where the wall aspect ratio is less than or equal to approximately 1, and for which the loading is cyclic. Lateral deflections at ultimate load, and at points in the softening region beyond ultimate, are obtained and converted to drift information. The statistical nature of the data is also investigated. These data are shown to be lognormally distributed, and an analysis of variance is performed. The use of these statistics to estimate Probability of Failure for a shear wall structure is illustrated.

1 INTRODUCTION

Low-aspect-ratio reinforced concrete shear (or "structural") walls are common structural elements found in nuclear reactor buildings. When properly designed, these walls possess characteristics of stiffness, strength, and ductility that are favorable for withstanding lateral seismic loads. Shear walls used in protective structures are typically stiff and, therefore, tend to prevent the large deformations that can be a problem for attached nonstructural components. However, under sufficient lateral seismic excitation, these walls can fail by a variety of mechanisms (Farrar, et al., 1993), resulting in significant lateral displacements and loss in stiffness and strength.

Because of the potential hazards, sophisticated analysis procedures have been developed over the past 20 years to quantify the probability of failure of nuclear power plant structures. Two such procedures (Reed & Gurbuz, 1993) are seismic probabilistic risk assessments (SPRA) and seismic margins assessments (SMA). SPRA is a formal process by which the uncertainty and randomness in various physical parameters (seismic input, response, and structural capacities) are propagated through an engineering analysis to generate a probability distribution for frequency of occurrence of failure. SMA (closely related to SPRA) establishes an earthquake level at which there is a high confidence of low probability of failure for the structure.

For a shear wall, the ultimate drift limit is defined as the lateral displacement at the top of the wall relative to its base, which corresponds to some definition of structural failure, normalized by the height of the wall. When performing SPRAs and SMAs, an accurate (rather than conservative) estimate of the ultimate drift limit is needed to estimate the inelastic seismic capacity of concrete protective structures (Reed & Gurbuz, 1993). In many investigations, loss of function for equipment housed within these structures has been considered to occur when the ultimate drift limit is reached; hence, the ultimate drift limit is a failure parameter in these studies.

The objective of this study is to establish the appropriate values of ultimate drift limit and the associated statistics of this parameter for potential use in the SPRAs and SMAs. Because the results of this work will be used to assess the inelastic seismic capacity of nuclear power plant structures, attention is focused on lightly reinforced (<1%) shear walls with low aspect ratios (less than or equal to approximately 1).

2 DRIFT DATA SUMMARY

Numerous experimental studies on shear walls laterally loaded beyond the elastic range that have been reported over the past 40 years are summarized in Duffey, et al., 1994. However, many of these studies present data only up to the ultimate (maximum) load capacity of shear walls. Efforts at recording the load-displacement behavior beyond this point have been more limited. Nonetheless, useful energy-absorption capability may exist beyond the point of maximum load resistance; and displacements may still be sufficiently small that the attached nonstructural components do not fail. In Duffey, et al., 1994, fifty studies were screened for pertinent drift data. Drift data were taken from those papers containing data beyond ultimate load for which shear wall aspect ratios were approximately one or less and for which walls were subjected to cyclic loading. Loading was displacement controlled in most instances.

So that drift data are obtained from the various references in a uniform manner, a data reduction procedure was developed and applied to the data in the literature in a consistent manner. Details of the data reduction procedure, including the handling of special cases, are presented in Duffey, et al., 1994.

Care must be exercised in using drift values beyond ultimate load (i.e., in the softening region), because relatively little resistive energy may remain in the structure, although the energy remaining in the earthquake input may still be significant. It should also be mentioned that the limiting factor for lateral drift of shear walls may be damage to attached nonstructural components, such as piping. The drift that such nonstructural components are capable of withstanding is component specific (Farrar, et al., 1993), and it appears unlikely that a meaningful general limit could be deduced from consideration of these components themselves. The drift at 100 percent of ultimate load therefore is the most appropriate definition of ultimate drift limit when used in conjunction with hysteretic models for nonlinear time-history analysis in seismic SPRAs (Kennedy, et al., 1988).

3 STATISTICAL ANALYSIS OF THE DATA

Basic statistical results from the previous section are plotted in Figure 1, where the sample mean, median, and range are seen to increase monotonically as the lateral load decreases beyond its ultimate value. Histograms showing the ranges and distributions of geometrical and material properties of shear walls used in these studies can be found in Duffey, et al., 1994.

3.1 Drift statistics by experimenters

More detailed statistical analyses were performed using a commercial statistical analysis software package [SAS, 1985]. The first study compares the drift limits obtained by each experimenter for the case of drift at 100 percent of ultimate load. Results presented in Table 1 include the mean drift, coefficient of variation, and the approximate lower 95 percent confidence limit for each of the experimenters. In Table 1, the Coefficient of Variation is the standard deviation divided by the mean, i.e., a relative standard deviation. The Lower 95 percent Confidence Limit (one tail) is that value of drift for which one is 95 percent certain that the actual mean is greater. Note that in constructing Table 1, all results of a given experimenter have been combined.

TABLE 1 Drift Statistics by Experimenter for Drift at Ultimate Load			
Experimenter, (See Duffey, et al., 1994)	Mean Drift (%)	Coefficient of Variation	95% Confidence Limit, Drift (%)
Shiga (1973, 1976)	0.45	0.25	0.40
Endo (1982)	0.68	0.40	0.58
Pauley (1982)	0.55	0.26	0.41
Alexander (1973)	0.73	0.15	0.60
Ogata (1984)	1.00	*	*
Wiradinata (1986) Saatcioglu (1991, 1993)	1.29	0.48	0.99
Barda (1972)	0.83	0.54	0.53
* Always reported as 1.00% drift			

3.2 Combined drift statistics

The results of an analysis of variance for the data obtained by the methods of Section 2 are presented in Table 2. The standard deviations for the data are calculated based on a logarithmic transformation . Medians are also presented in Table 2, because the median is a better measure of central tendency for the lognormal distribution than the mean.

In Table 2, random standard deviations are a weighted average of those within a given investigation (i.e., "Experimenter," Table 1). Weights are assigned based on the number of experiments performed using a procedure described in Greybill, 1961. They are a measure of the average variation of the drift limit about the mean of the data for a particular experimenter. Systematic standard deviations are a measure of the average variance of means between experimenters. Systematic variation is attributed to bias caused by the inability of experimenters to establish their experimental program and measurement procedures in precisely the same way. The statistical models used make the idealization that within a given investigator's set of experiments no systematic error occurs. The systematic error within a given investigation is believed small in comparison to the systematic error between investigators. Composite standard deviations are obtained from the square root of the sum of the squares of random and systematic standard deviations. Note that another study (Kennedy, et al., 1988) has shown a composite standard deviation similar to the value generated in this study (Table 2), although random standard deviations were considerably lower and systematic standard deviations were correspondingly higher.

Also shown in Table 2 are upper and lower 95% confidence limits on the composite log standard deviations. The limits were obtained using Greybill, 1961, and Welch, 1956. The limits were computed as a function of the random and systematic standard deviations as well as tabulated values of the Chi-Square distributions with degrees of freedom given as a function of the number of experimenters and the number of data points.

It is noted from Table 2 that the systematic log standard deviation for drift at ultimate load (100%) appears low in comparison with data at other fractions of ultimate load. Further, the composite log standard deviation monotonically increases as the load fraction decreases beyond ultimate load. These observations are expected because the response in the softening region is more difficult to measure and is subject to random variability caused, in part, by the stochastic nature of concrete cracking.

A comparison of the combined statistics for the original data (i.e., without the log transformation) can be found in Duffey, et al., 1994.

TABLE 2 Median and Associated Logarithmic Standard Deviation						
Percent Ultimate Load (%)	Median (%)	Random Log Std. Dev.	Systematic Log Std. Dev.	Composite Log Std. Dev.	Uncertainty in Composite Log Std. Dev. Lower 95%	Upper 95%
100	0.72	0.35	0.13	0.373	0.330	1.04
90	1.00	0.28	0.33	0.437	0.286	0.919
80	1.24	0.29	0.35	0.452	0.297	0.949
70	1.48	0.28	0.37	0.464	0.304	0.986
60	1.64	0.30	0.43	0.524	0.370	1.34
50	1.84	0.24	0.51	0.566	0.332	1.59

3.3 Investigation of Distribution Type

The Wilk-Shapiro W-Test (Shapiro and Wilk, 1965) was used to determine that the data were lognormally distributed. A comparison of the data for 100 percent load with the lognormal fit is shown in Figure 2 (a plot of the drift limit data [in log form] as a function of the number of standard deviations from the mean). The straight line shown in Figure 2 corresponds to a lognormal fit. The lognormal distribution fits the data well from -1 standard deviation to +2 standard deviations. Deviations from the lognormal distribution are observed at the lower tail below -1 standard deviation. For most seismic hazard zones, the lower tails of the fragility curve will have less than a 5 percent effect on the overall probability of failure estimate (Ravindra, et al., 1984). Therefore, the lognormal assumption is reasonable for the 100 percent load data despite the lack of fit at the lower tail.

4 PROBABILITY-OF-FAILURE ESTIMATION

To incorporate the ultimate drift limit data into a SPRA or SMA, the drift limit statistics must be transformed into a fragility curve. This curve gives the structure's probability of failure as a continuous function of some measure of ground motion level, typically peak spectral acceleration, and is structure specific. A detailed example of the procedure to transform the drift limit statistics into a fragility curve can be found in Kennedy, et al., 1988. This procedure is outlined below.

The first step in the procedure to develop a fragility curve is to establish a probability distribution function for failure as a function of maximum story drift. As discussed in Section 3, statistical analysis of the data summarized in the current study shows that a lognormal distribution is valid.

Next, the probability of failure, P_f, is estimated using a logarithmic standard deviation based solely on random variability of the shear wall ultimate drift limit, β_R. Randomness of ground motion is incorporated by using results from sets of nonlinear, deterministic, time-history analyses that use different inputs normalized to selected peak spectral acceleration values, $\overline{S}_a$, within a frequency range of interest. All analyses utilize median structural properties. To estimate P_{f_i}, the probability of failure for the ith analysis, drift values calculated for all walls in the time history structural analyses are screened to determine the maximum calculated percent story drift. The number of standard deviations that the calculated maximum drift is from the median ultimate drift limit can be computed as

$$x = \frac{\ln\left(\frac{\delta_c}{\delta_m}\right)}{\beta_R} \qquad (1)$$

where x = the number of standard deviations from the median, δ_c = the maximum calculated drift, and δ_m = the median drift limit obtained from the experimental data.

P_{f_i} can now be determined from the cumulative distribution function for a normally distributed random variable as

$$P_{f_i} = \int_{-\infty}^{x} \frac{1}{\sqrt{2\pi}} e^{-0.5t^2} dt \tag{2}$$

where t is a variable of integration. The mean probability of failure, P_f, from all structural analyses corresponding to a particular value of $\overline{S}_a$ is next determined by averaging P_{f_i} from all analyses.

A median fragility curve, based on random variability only, can now be developed. A lognormal distribution is fit to the values of P_f determined for the various spectral acceleration levels used in the time-history analyses. This distribution provides a continuous function for the probability of failure versus the peak spectral acceleration. From this fit a median spectral acceleration level that will produce structural failure and a logarithmic standard deviation that considers random variability only can be obtained.

The probability of failure based on the composite lognormal standard deviation which considers both randomness and uncertainty is determined in a similar manner as the probability of failure that considers random variability only. Analyses are again performed (at various spectral acceleration levels) that account for uncertainties in structural properties such as shear wall stiffness, strength, and damping. Estimates of the probabilities of failure are determined from these analyses.

Again, a lognormal fragility curve, this time based on composite variability, is developed by fitting a lognormal distribution to the probability of failure data that is given as a function of $\overline{S}_a$. Using the previous β_R, the value of the lognormal standard deviation that considers systematic variability only, β_U, can be determined as

$$\beta_U = \sqrt{\beta_c^2 - \beta_R^2} \tag{3}$$

A spectral acceleration value corresponding to a high confidence of low probability of failure (HCLPF, 95 percent confident that there is less than a five percent probability of failure) can be determined from the assumed lognormal distribution as

$$\text{HCLPF} \quad \overline{S}_a = \text{Median}\left(\overline{S}_a\right) e^{-1.65(\beta_R + \beta_U)} \tag{4}$$

Finally, the fragility estimates are revised to reflect other sources of variability related to modeling, directional effects, and incoherence of ground motion not accounted for in the nonlinear analyses. Inclusion of these effects is illustrated in Kennedy, et al., 1988.

5 CONCLUSIONS

1. Screening of 50 references containing shear wall experimental data led to the selection of ten references containing relevant data for shear walls with aspect ratios of approximately 1 or less undergoing cyclic loading. These low aspect ratios are common for shear walls found in protective structures. Further, cyclic loading is relevant to seismic response.
2. A total of 69 data sets were obtained graphically from these papers using a set of rules established in Section 2. The rules provide lower-bound estimates for drift at ultimate load. Drift limits at ultimate load and beyond (at 90, 80, 70, 60 and 50 percent of ultimate load) were determined and their statistical properties were examined.
3. The data were found to be lognormally distributed and the use of these statistics to estimate the probability of failure of a shear wall structure was outlined.

ACKNOWLEDGMENTS

This work was sponsored by the U. S. Nuclear Regulatory Commission Office of Nuclear Regulatory Research, Division of Engineering, Mr. Roger M. Kenneally program manager. The results presented do not necessarily represent the NRC's position on this subject.

REFERENCES

Duffey, T. A., A. Goldman, & C. R. Farrar 1994. "Shear Wall Ultimate Drift Limits," NUREG/CR-6104, U. S. Nuclear Regulatory Commission, Washington, D. C.

Farrar, C. R., J. W. Reed, & M. W. Salmon 1993. "Failure Modes of Low Rise Shear Walls," *ASCE Journal of Energy Engineering*, 119: 119-138.

Kennedy, R. P., D. A. Wesley, & W. A. Tong 1988. "Probabilistic Evaluation of the Diablo Canyon Turbine Building Seismic Capacity Using Nonlinear Time History Analyses," NTS Report No. 1643.01.

Ravindra, M. K., H. Banon, R. H. Sues, & R. D. Thrasher 1984. "Sensitivity Studies of Seismic Risk Models," Electric Power Research Institute report NP-3562.

Reed, J. W., & O. Gurbuz 1993. "Introduction to Structural Failure Modes for Nuclear Power Facilities," *ASCE Journal of Energy Engineering*, 119: 75-81.

SAS User's Guide: Statistics, Version 5 Ed., SAS Institute, Inc., Carey, NC, 1985.

Graybill, F. A. 1961. *An Introduction to Linear Statistical Models*, Vol. 1, McGraw-Hill, NY.

Shapiro, S. S., & M. B. Wilk 1965. "An Analysis of Variance Tests for Normality (Complete Samples)," *Biometrika*, 52: 591-611.

Welch, B. L. 1956. "On Linear Combinations of Several Variances," *Journal of the American Statistical Association*, 51: 132-148.

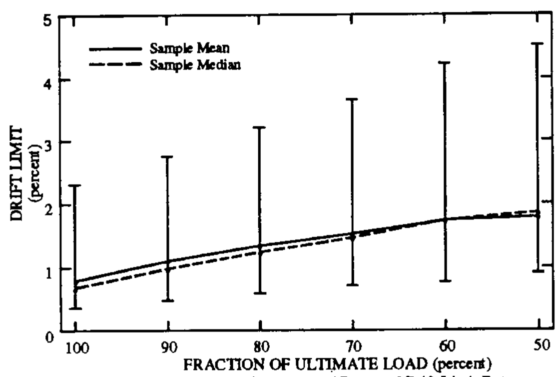

Fig. 1 - Central Tendancy and Range of Drift Limit Data

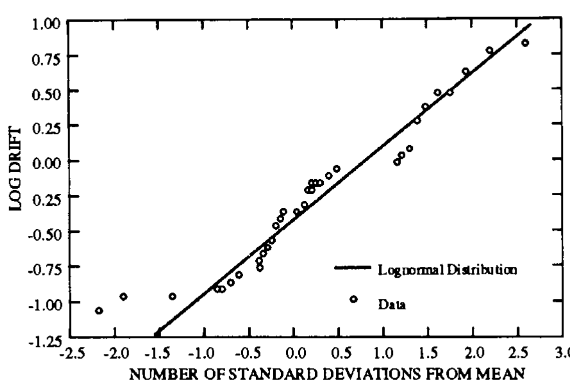

Fig. 2 - Log Frequency Plot